

# Comparative Spectral Analysis of Field Data from Schalkwijk Measurements and Simulated Axle Loads



www.tno.nl +31 88 866 20 00

TNO 2025 R11004 – 15 May 2025 Comparative Spectral Analysis of Field Data from Schalkwijk Measurements and Simulated Axle Loads

Author(s) Moretti D.
Classification report TNO Internal
Report text TNO Internal

Number of pages 34 (excl. front and back cover)

Number of appendices 0
Sponsor ProRail
Programme number IBS

Project name ProRail - Analyse Trillingspectra

Project number 060.61434/01.01.01

All rights reserved

No part of this publication may be reproduced and/or published by print, photoprint, microfilm or any other means without the previous written consent of TNO.

© 2025 TNO

#### **Contents**

1	Introduction	4
2 2.1 2.2	Data description and methodology	5 5
3	Results	13
3.1	Dynamic force spectra of the simulations VIRM SLT	15
3.3 3.4	All train types	21
4	Conclusions & Recommendations	28
5	References	30
6	Signature	31

#### 1 Introduction

Trian-induced vibrations and the relation with the status of the track and the train-type are a recurring topic for ProRail who is responsible for the maintenance of the railway system of the Netherlands.

The IBS research program (Innovatieagenda Bronaanpak Spoortrillingen), funded by ProRail, seeks to determine methods for reducing ground vibrations caused by railway traffic. Both infrastructure and train interventions are analyzed in terms of their effectiveness in reducing ground vibrations.

In the IBS program, the question has arisen whether the dynamic axle loads on the rail have a direct correspondence in terms of frequency content with measurements in the field away from the track. As a first step to address this question, ProRail has asked TNO to compare simulated dynamic axle loads with field measurements to investigate if there are any similarities in the frequency spectra. This report discusses the results of this study.

The field measurements used in this report are carried out by RIVM in the period between the 11<sup>th</sup> of October and the 7<sup>th</sup> of November 2018. The simulated axle loads, the so calle loads, originate from simulations by Ricardo, who assessed the dynamic load exerted on the railway track by various types of train equipment through multi-body dynamics simulations [1]. The track condition in these simulations is based on rail geometry measured at location Schalkwijk.

Comparison of the simulation results [1] with the field measurements is carried out in the frequency domain to check whether the modelled dynamic force spectra have a clear correlation with the measurement data. Also, trends identified in the spectral data with respect to train types and train speeds are reported.

Chapter 2 provides a description of the available experimental and numerical data and the methodology used to compare them. Chapter 3 discusses the results from the data analysis. The comparison of the numerical data with measurements, and the effect of train type and velocity on the measured vibrations. Finally, Chapter 4 outlines conclusions and recommendations.

) TNO Internal 4/34

## 2 Data description and methodology

In this chapter, the measurement and simulation data used for the analyses are described in detail.

#### 2.1 Schalkwijk Measurement Campaign

In the context of the development of a validation set for the OURS model, RIVM funded a number of measurement campaigns to gather calibration and validation data for the numerical model.

Among the measurement campaigns, the location in Schalkwijk has been monitored (approximate location: latitude 51.975346, longitude 5.198671) between 11<sup>th</sup> of October and the 7<sup>th</sup> of November 2018 by Cauberg-Huygen. Redbox triaxial geophones MR30 from SYSCOM were placed on 3x3 grid of sensors of approximately 25 m distance from each other and approximately 25 m distant from the tracks. For each train passage, the ground velocity at each of the 9 measurement points (MP1 to MP9) was measured in 3 orthogonal directions for a total of 27 time-traces available per train passage. The arrangement of the sensors and their distance to the track is shown in Figure 1 while a mapping from measurement point (convention in the figure) to sensor label is shown in Table 1.

Table 1 Mapping from measurement point to sensor label and corresponding distance from the tracks.

Measurement point	Sensor label	Distance from tracks [m]
MP1	MT30	25
MP2	MT31	25
MP3	MT32	25
MP4	MT33	49
MP5	MT34	49
MP6	MT35	49
MP7	ZT42	72
MP8	ZT44	72
MP9	ZT45	72

) TNO Internal 5/34

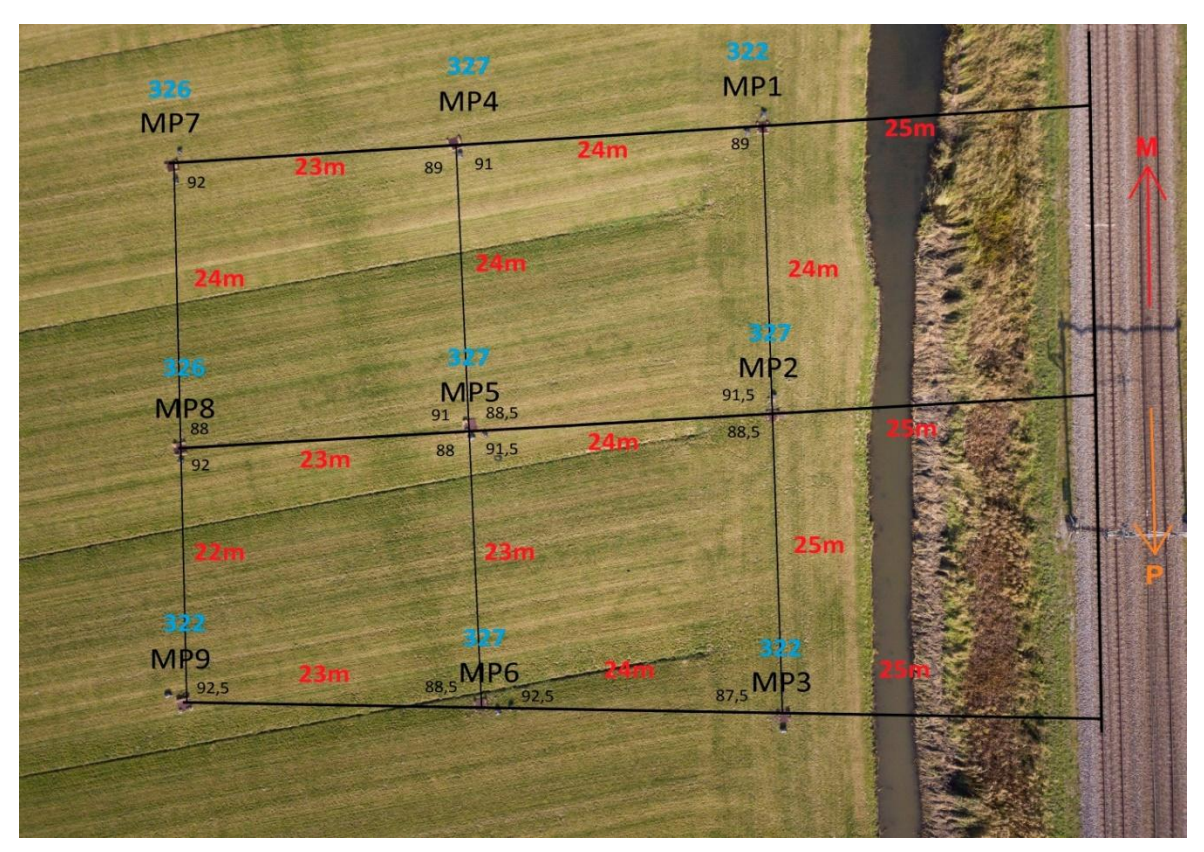


Figure 1 Arrangement of the sensors and their distance to the track for the Schalkwijk measurement campaign.

The data have been shared in a Proprietary Software Format XMR, which is direct output of the SYSCOM geophones in binary format. An accompanying MATLAB reader has been used to read the data into Python after appropriate conversion.

The data of the passage is stored by sensor, each of which measures a "train passage" when a certain threshold velocity is exceeded. The filename of each passage stored by a sensor differs per sensor. An excel file was provided that maps each unique train passage to the corresponding file name per sensor. The structure of the excel file is a table providing, per train passage, the following information:

- Train type
- Train speed (km/h)
- Direction
- Filename per sensor and relative path of the file

Figure 2 provides the count of train passages per each unique train type label provided in the excel file. It should be noted that no other information or description is provided for each of the train labels defined for the train types, hence some of the traces have been discarded because of the lack of train type information. The number of discarded passages is very small (21, 0.5% of the total) and does not affect the analysis.

) TNO Internal 6/34

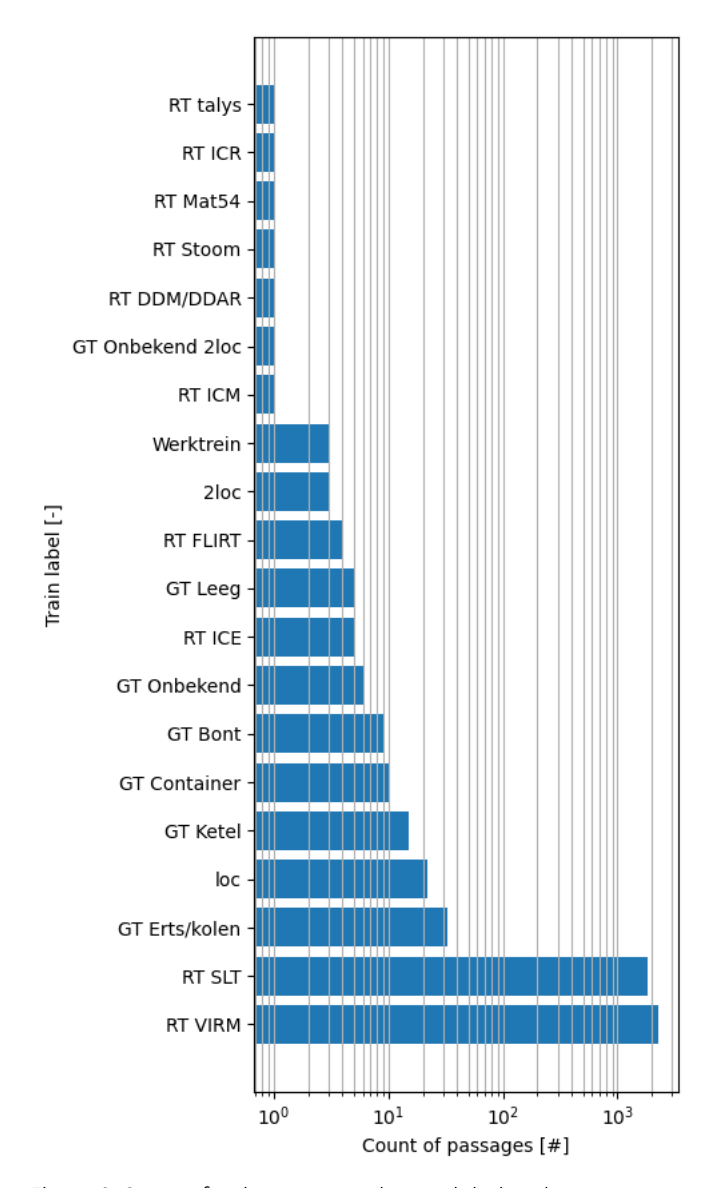


Figure 2 Count of train passages observed during the measurement campaign of Schalkwijk between the 11<sup>th</sup> of October and the 7<sup>th</sup> of November 2018 divided per train type in log-scale where the train type is provided in the measurement documentation.

To perform relevant and sound statistical analyses, a relatively large number of passages is required. Only train types with more than 20 passages have been considered. Besides this, the freight trains (GT) have been grouped together. Table 2 provides a tabulated count of passages per train type divided into different speed intervals for the train types with at least twenty passages. From table 2 and figure 2, the following is concluded:

- The count of passages measured for SLT and VIRM per speed interval is significant and large enough to perform further analysis also when dividing the measurements in speed intervals
- The number of passages of and loc, which is assumed to be single locomotives, is limited and therefore only limited information can be drawn from the measurements.

TNO Internal 7/34

Table 2: Count of train passages observed during the measurement campaign of Schalkwijk between the 11<sup>th</sup> of October and the 7<sup>th</sup> of November 2018 divided per train speed interval and grand total (right column).

Train	50-70	70-90	90-105	105-115	115-125	125-135	Total	
GT*	2	56	20	0	0	0	78	
SLT	0	9	60	313	909	556	1847	
VIRM	1	40	138	397	1072	646	2294	
Loc**	0	5	10	3	2	2	22	

<sup>\*</sup>GT stands for various "Goederentreinen" (freight trains)

The available time-traces have been converted to power-spectral density (PSD) using the Welch estimator [2]. Because the passages are characterized by a varying duration, a number of frequency lines is specified in the Welch estimator so that the PSDs of all the passages have the same frequency lines and can be compared to each other. In particular, the number of frequency lines is 65536 with one segment and a Hamming window [3].

As an example, train passage 125 from a VIRM train is presented in Figure 3. This train has a speed of 103km/h. Shown are results for the closest sensors to the tracks (MT30, MT31, MT32) for the vertical component of the ground velocity ( $V_z$ ).

) TNO Internal 8/34

<sup>\*\*</sup>Number of passages with single locomotives

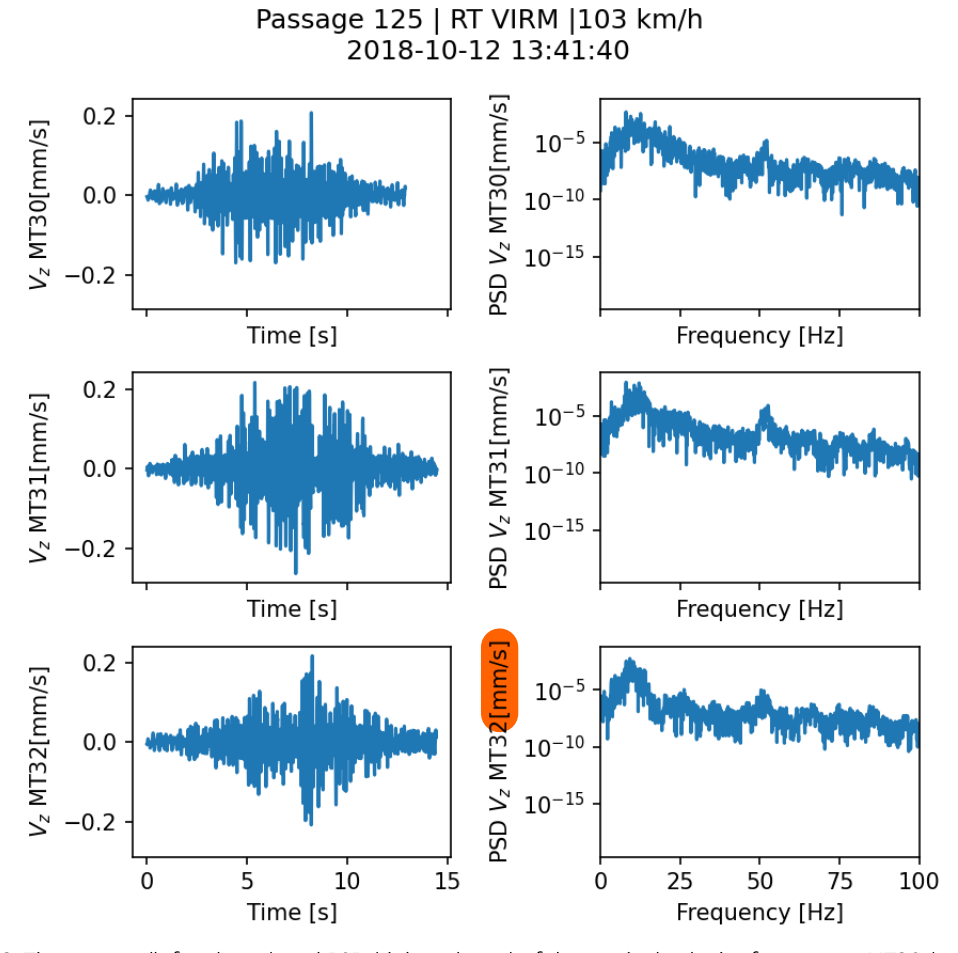


Figure 3: Time -trace (left column) and PSD (right column) of the vertical velocity for sensors MT30 (top), MT31 (middle) and MT32 (bottom) for passage ID 125 of VIRM train at about 103 km/h.

From the figure, it is seen that even for sensors located at the same distance from the track, 25 meters from each other, and for the same train passage, a variability is found in the response. To detect common trends in each receiver, the median and average PSDs have been computed from the ensemble of passages for different train speed intervals.

Figure 4 shows the ensemble of PSDs obtained from VIRM train passages between 90 and 110 km together with the mean (red) and median (black) PSD obtained from 256 passages for sensor MT32 (vertical velocity).

The median and mean PSD can highlight whether a pattern can be found in the measured vibration by averaging over a sufficient number of samples.

) TNO Internal 9/34

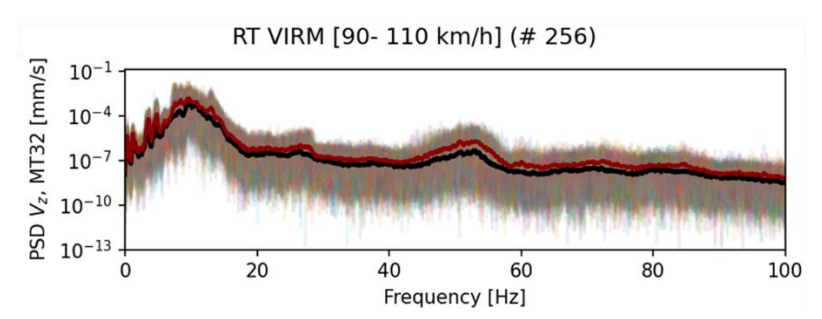


Figure 4: Example of the ensemble of PSD of the vertical velocity obtained from multiple (256 in this case) measure a train passages (background lines) and median (black) and mean (red) PSD from the ensemble for a speed interval of 90-110 km/h and sensor MT32.

To observe whether a variation of the frequency content over time is observed during the train passage, the use of spectrograms was also explored. Spectrograms show time on the x-axis, frequency on the y-axis, and the color at each time-frequency point shows the amplitude. Such technique is appropriate to investigate the frequency content for transient vibration sources where the distribution of the power per frequency of the signal can change over time.

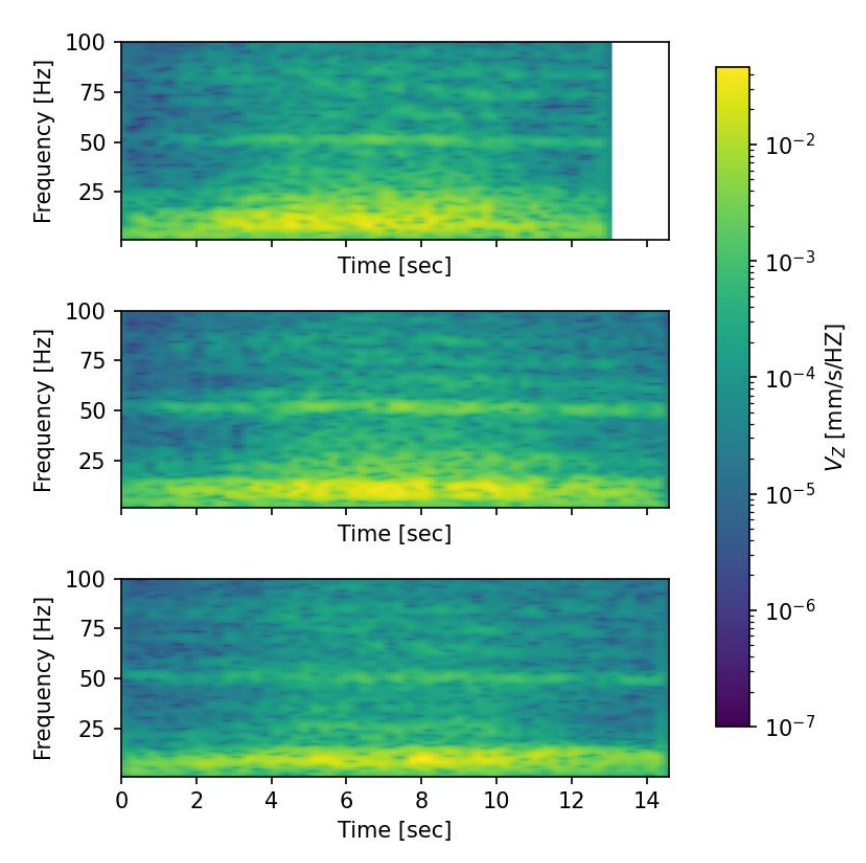


Figure 5: Spectrogram of the vertical velocity for sensors MT30 (top), MT31 (middle) and MT32 (bottom) for passage ID 125 of VIRM train at about 103 km/h.

Figure 5 shows the spectrogram of passage 125 (103km/h) with the color scale in log-scale. As can be seen from the figure, the frequency content observed by the overall PSD are approximately horizontal lines in the spectrogram. There are no doppler-like effects observed

where the frequency is higher when the train approaches the sensor and lower when the train is moving away from the sensor. Typically, the Doppler effect can lead to significant shift in frequency content: for a shear wave velocity of the soil of 200m/s and train speed of 27.7m/s (100km/h), a doppler effect would lead to an increase of 15% of the peak frequency which should clearly be visible in at the edges of the spectrogram in the range of 50Hz. Because such effect is not clearly visible in the spectrogram, such analysis technique is not further pursued.

#### 2.2 Simulation of train-induced loads

In the report provided by Ricardo [1], train loads are simulated by letting a train model pass on a track with a given speed. Ricardo has investigated different train speeds for different train types while also using measured Schalkwijk track conditions (track irregularity) in the simulations.

In each simulation, the trains drive virtually with a certain speed over a track characterized by track irregularities. From the simulations, the reaction forces induced by the train vehicles (more specifically the wheel-rail forces), are computed and provided in terms of the PSD. These forces are being regarded as the dynamic load responsible for the ground vibrations and are compared with the field measurements discussed in the previous paragraph.

Three tracks were used for the simulations: a synthetic track where the vehicle is nudged with broadband, a track from practice (realistic track) and a track with a short-wave defect. For the train models, 11 train types are considered: 2 freight wagons (empty and loaded), 3 locomotives and 6 types of passenger trains. The results of the simulations are used to discuss possible measures to mitigate vibrations where dynamic load is the highest.

A number of different train types have been modelled in [1]: freight trains (Falns), Passenger trains (RT: VIRM, DDZ, SLT, ICM) and locomotives (Traxx, Loc1700 and Class'66).

The combination of train type and train speed simulated by Ricardo is presented in Table 3. From the individual PSD of each axle, an average PSD is computed (4 axles). Figure 6 shows an example the PSD of the four individual axles for the Falns Y25 Max Basis at 100 km/h.

The results of the analyzed train speed and train type combinations on the realistic track have been provided by Ricardo for the realistic track in form of a file containing the PSD of the dynamic load, averaged over the axles, and with a frequency up to 100Hz.

Table 3 Combination of train types and train speed performed by Ricardo, from [1].

Voertuigtype	40 km/u	80 km/u	100 km/u	120 km/u	140 km/u	160 km/u
Falsa V25 Laas/baladas				(I)		
Falns Y25 Leeg/beladen	X	X	X	x (Leeg)		
Falns 3-piece Leeg/beladen	X	×	X	x (Leeg)	•	-
Class'66 locomotief	X	X	X	X	-	-
Loc1700 locomotief	X	x	X	x	X	-
Traxx locomotief	X	X	X	X	X	-
VIRM mBvk1 leeg	X	x	X	X	X	-
ICMm mBFk leeg	x	X	X	X	X	X
DDZ ABvk leeg	X	X	X	X	X	-
SLT 4-baks leeg	X	X	X	X	X	X
SNG 4-baks leeg	X	X	X	X	X	X
Flirt IV leeg	X	X	x	X	X	-

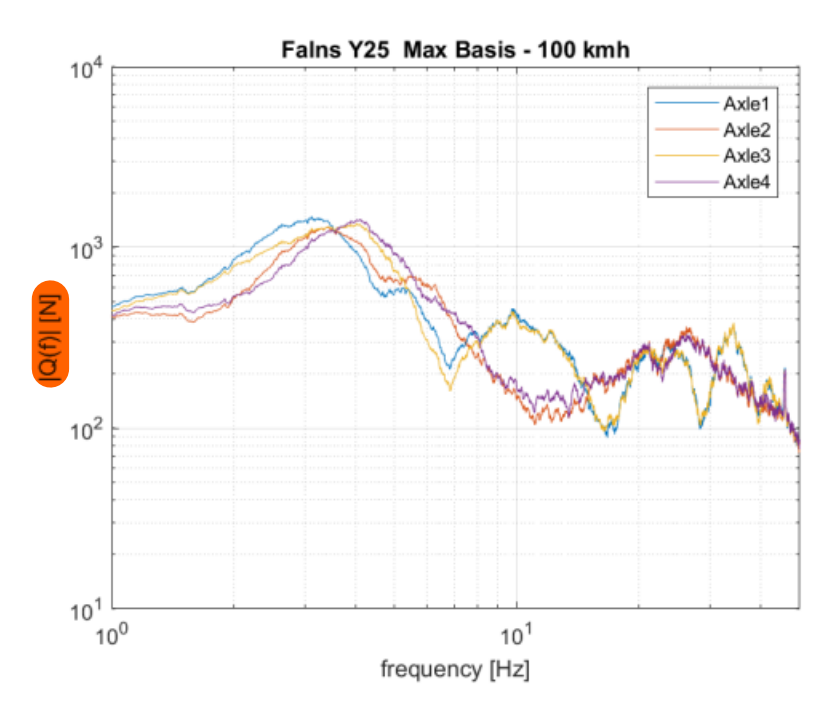


Figure 6: Example of power spectral density of the wheel-to-track contact force for each of the axles in the simulations of Ricardo for one train configuration (Falns Y25, freight train at 100 km/h), from [1].

) TNO Internal 12/34

#### **3** Results

This chapter discusses spectral analyses for each train type and analyses how train speed affects measured vibrations.

For the evaluation of the dependency between train-speed and measured frequency content, the train passages have been divided into intervals of train speed of respectively 90, 105, 115, 125, 145 km/h. For each interval of train speed, the median and mean PSD obtained from the ensemble of PSDs is evaluated and compared with the dynamic force spectra from Ricardo. The analyses above have been carried out for the VIRM and SLT train passages, since for those a sufficient amount of passage was recorded during the measurement campaign to estimate accurately median and mean PSD from the ensemble of PSDs.

#### 3.1 Dynamic force spectra of the simulations

In this section, the simulated dynamic force spectra are investigated without comparing to field measurements. Dependency with speed and similarities and differences with train type are studied. This facilitates understanding of the results when comparing with measurements.

Figure 7 and Figure 8 shows the PSD of the Q Force for passenger cars (SLT and VIRM), a Traxx locomotive and a Falns freight train simulated by Ricardo [1] and different train speeds. In Figure 7 the PSD's are grouped by train types (with varying speed) while in Figure 8 the PSD's are grouped by train speed (with varying train types).

In the PSD of the simulations, a trend of increasing frequency content and a shift in frequency peak is observed for both train types. For the sleeper passing peaks of the spectra (46 Hz, 55 Hz and 64.5 Hz), it can be observed that with increasing train speed, the general power of the peak doesn't increase as the rest of the spectra and it also broadens, becoming relatively less pronounced. For the 140km/h speeds, the amplitude of the sleeper passing peak is hardly visible. It should also be noted that the amplitude of the sleeper passing frequency doesn't change with the train type used in the simulation.

The frequency slope after 20-30Hz is similar for the different train types, although it shifts to higher frequencies with increasing train speed.

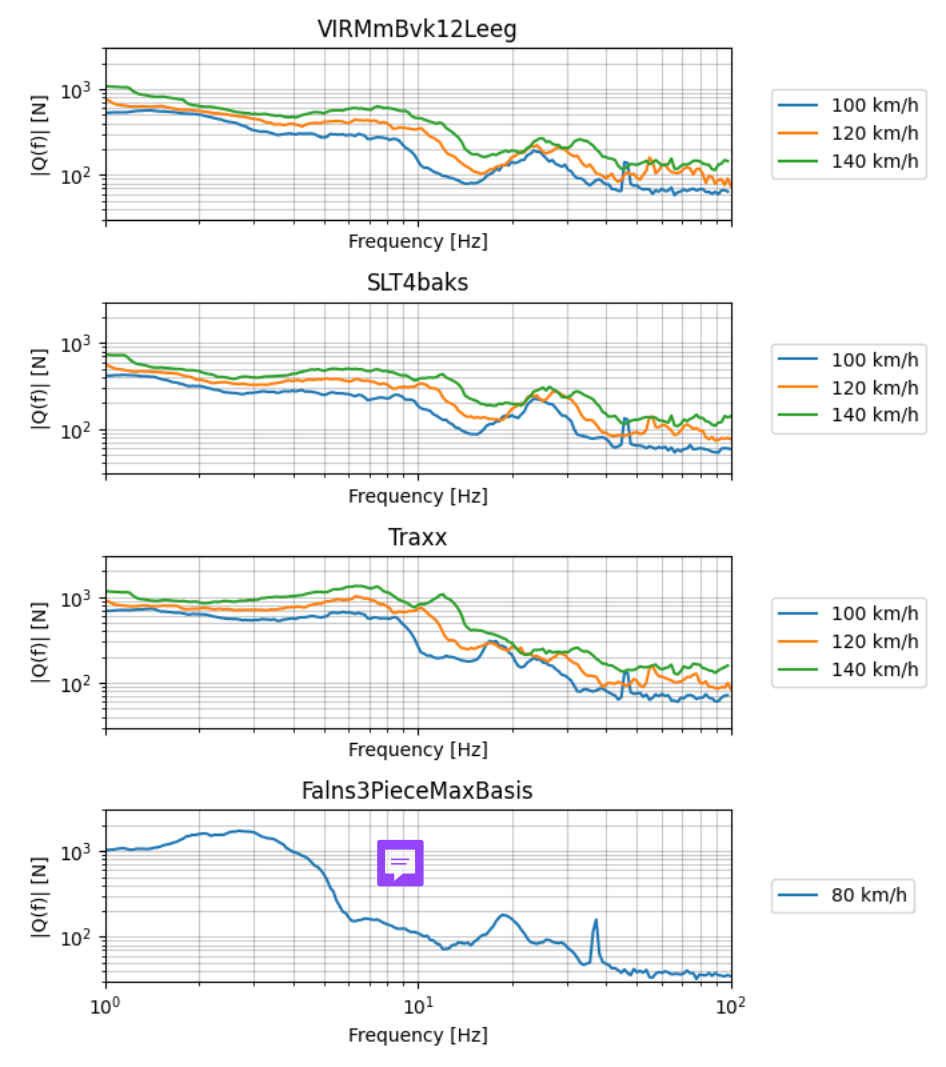


Figure 7: PSD force obtained from Ricardo for the VIRM (first row), SLT (second row), Traxx locomotive (third row) and, Falns freight train (fourth row) trains for different train speeds (colours).

) TNO Internal 14/34

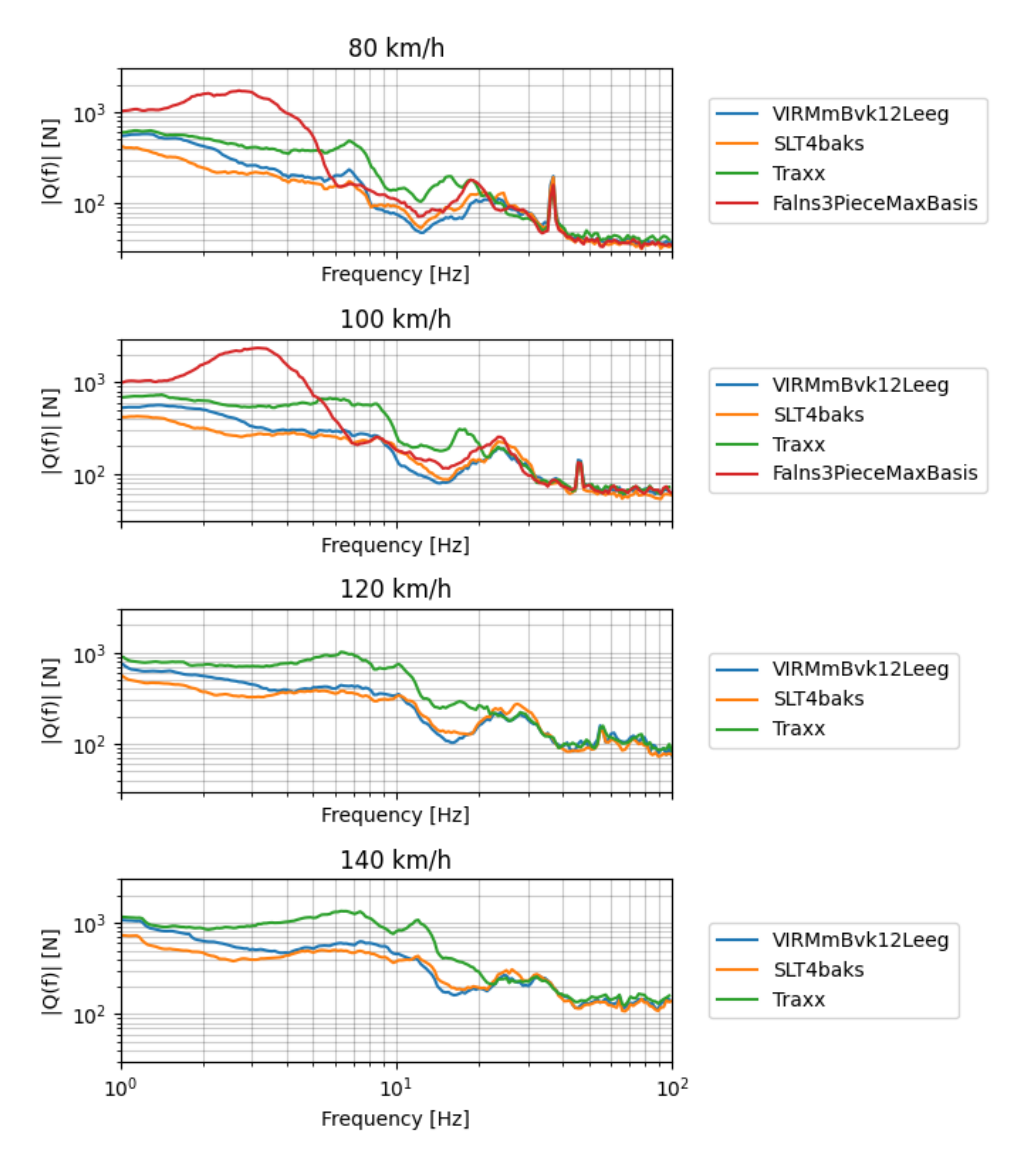


Figure 8: PSD force obtained from Ricardo for the 80 km/h (first row), 100 km/h (second row), 120 km/h (third row) and 140 km/h for different train types (colours).

#### 3.2 VIRM

Figure 9 show the median PSD obtained from the measurements (left y-axis) against the PSD force obtained from Ricardo (right y-axis) for the VIRM train for different intervals of train speed (rows). Note that there was not a matching Ricardo simulation for the speed interval 105-115 km/h.

In the figure, the row of sensors closest to the source, at about 25 m distance, is used (MT30, MT31, MT32). If there is any correlation with the dynamic track loads it is most likely found in the sensors closest to the track. Figure 10 shows a comparison per sensor of the PSDs obtained per speed interval, while Figure 11 and Figure 12 provide a zoom on respectively the frequency content below 8 Hz and above 40Hz.

From the figures the following is observed:

- In comparing the sensors amongst each other, the median PSD is in good agreement in some parts of the spectrum, for example between 3-7Hz and between 50-70Hz
- In all sensors, the maximum response is found for frequencies between 8-15 Hz, but larger variability in the response is found as well as different attenuation between 15-30Hz which is likely related to local conditions at the sensor or in the path from the track to the sensor.
- For all sensors, a similar trend in amplitude and increase in frequency (shift to higher values with increasing train speed) is found. It is worth noting that the shape of the spectra between 8Hz and 40Hz shows a smaller dependency on the train speed.
- When the PSD of the dynamic load on the track resulting from the simulations (black line, right axis) is qualitatively compared with the output PSD, some similarities can be found in the relatively high-frequency range, but the peaks not always align. The simulated and measured frequency peak are compared to the upper and lower bound of the theoretical sleeper passing frequency, computed using the upper and lower bound of the speed intervals and assuming a sleeper distance of 0.6m. The theoretical range and the experimental peaks are tabulated in Table 4. All the experimental peaks are found at frequencies higher than the upper-bound of the theoretical sleeper passing frequency, except for the 125-135km/h speed interval. Interestingly, a relatively small amplitude is observed in the PSD of the dynamic force (140km/h), when compared to the sleeper passing frequency of 100 and 120 km/h.
- A poor match is found between the PSD of the force and the PSD of the velocities for the remaining part of the spectra, especially where the largest frequency content of the measurement is found (8-15Hz). Similarly to the VIRM, the experimental PSD shows in fact pronounced peaks which cannot be traced to peaks in the PSD of the force.

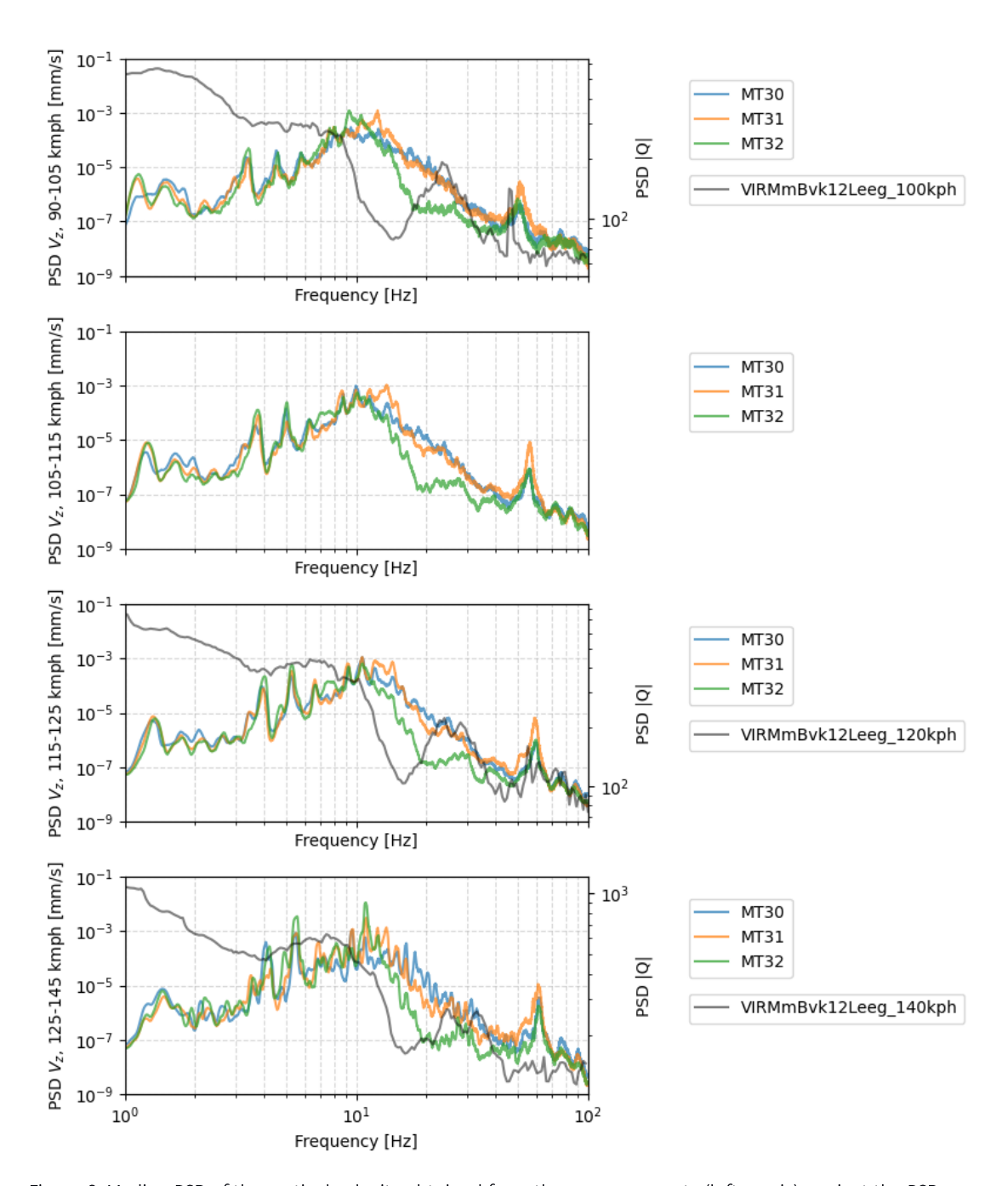


Figure 9: Median PSD of the vertical velocity obtained from the measurements (left y-axis) against the PSD force obtained from Ricardo (right y-axis, grey line) for the VIRM train for different intervals of train speed (rows). Note that there was not a matching Ricardo simulation for the speed bracket 105-115 km/h

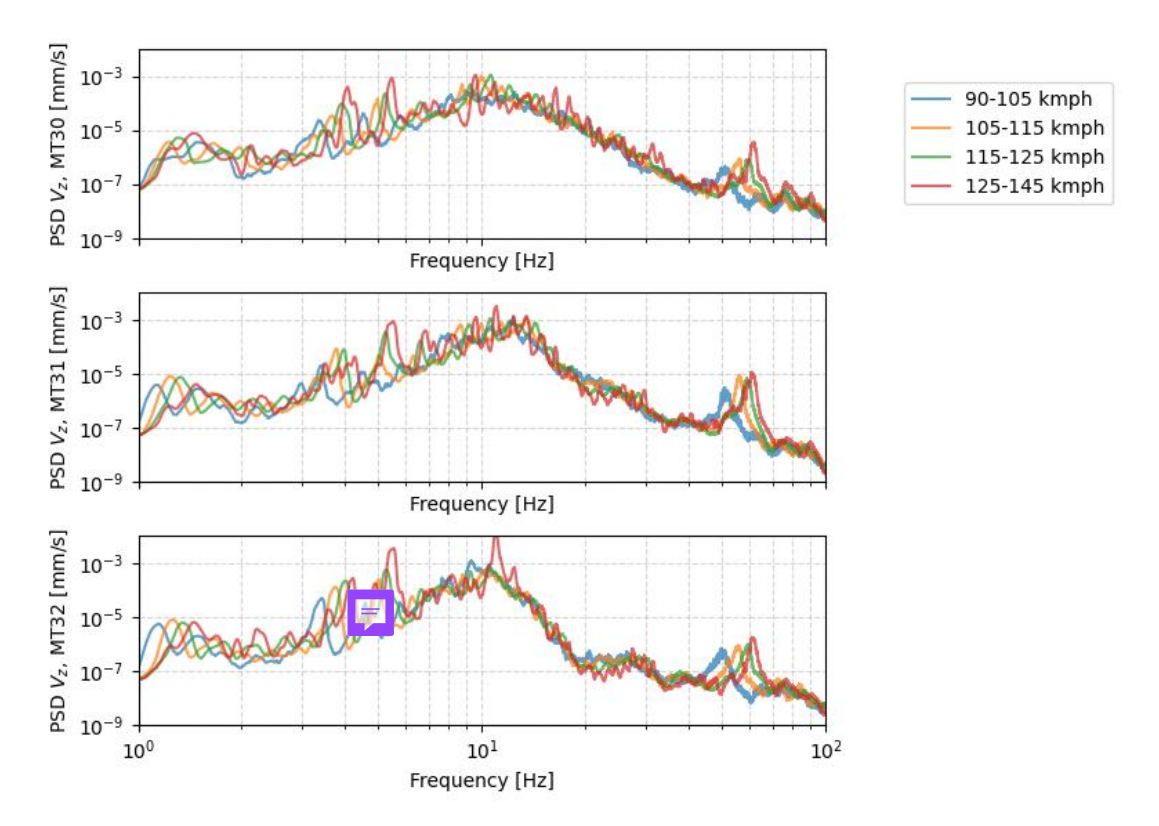


Figure 10: Median PSD of the vertical velocity for the sensors MT30 (top), MT31 (middle) and MT32 (bottom) for different VIRM train speed intervals (colours).

) TNO Internal 18/34

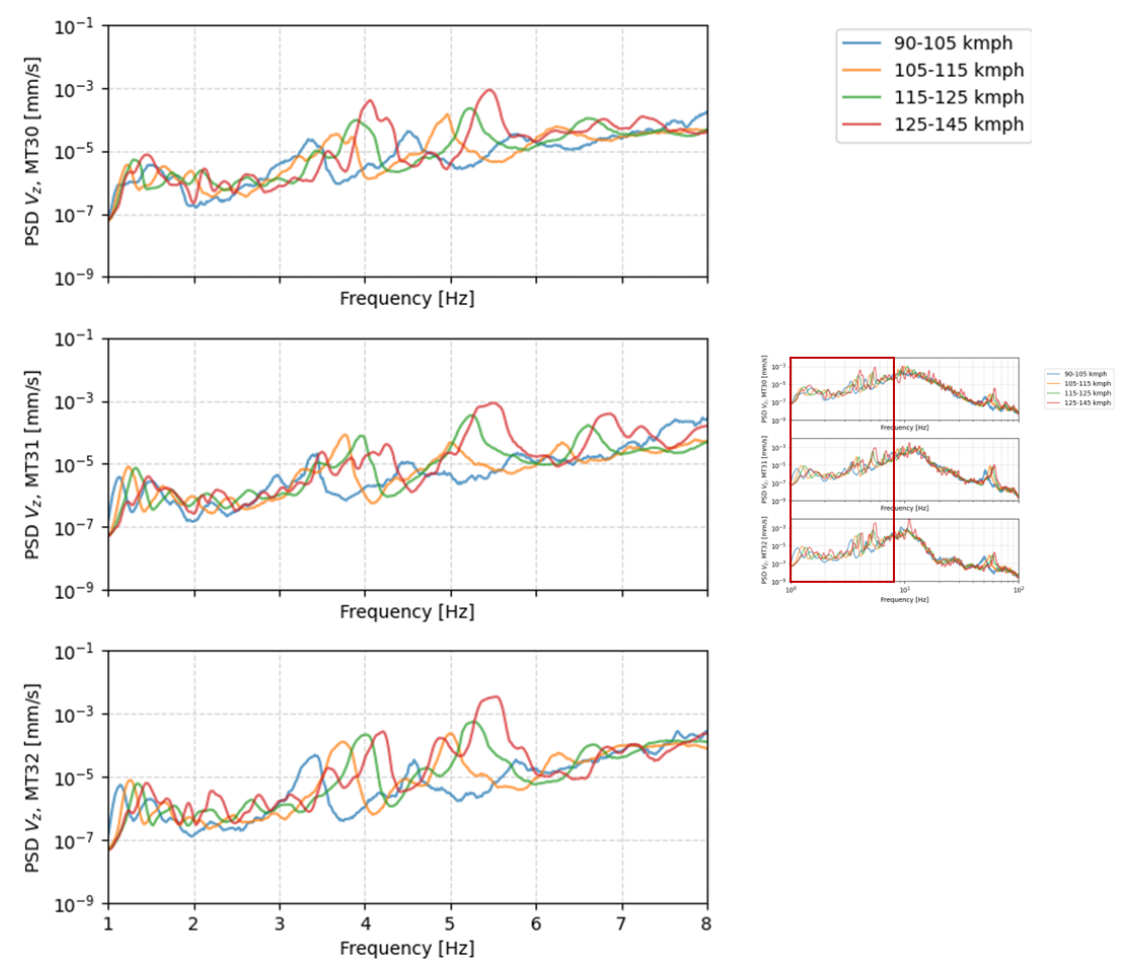


Figure 11: Median PSD of the vertical velocity for the sensors MT30 (top), MT31 (middle) and MT32 (bottom) for different VIRM train speed intervals (colours) zoomed in the range 1-8 Hz (see thumbnail on the right).

) TNO Internal 19/34

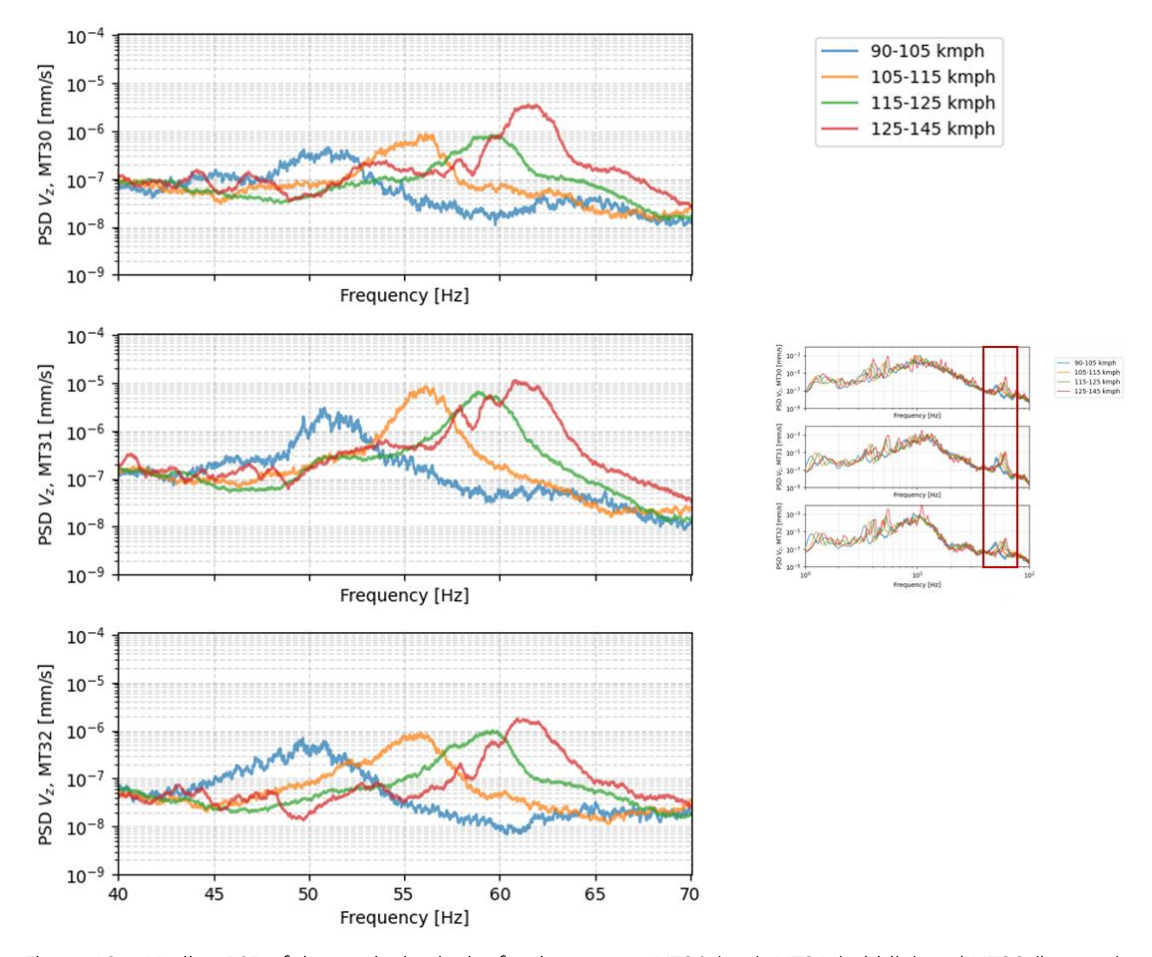


Figure 12: Median PSD of the vertical velocity for the sensors MT30 (top), MT31 (middle) and MT32 (bottom) for different VIRM train speed intervals (colours) zoomed in the range 40-80 Hz (see thumbnail on the right).

The difference in the low-frequency range (below 8 Hz) between the force PSD and measured PSD can be explained by the mobility lines, i.e. the transfer function between the ground velocity at a receiver in the field and the input force on the track. One example of a transfer function obtained from literature [4] is shown in Figure 13. From the figure, it can be seen that it's quite hard to produce amplitudes in the range below 7 Hz because of the small receptance of the

Table 4: Theoretical frequency range of the sleeper passing frequency from the measurement speed intervals assuming 0.6m sleeper distance against the experimental peak frequencies obtained from the VIRM train type and the sleeper passing peak simulated in [1] including the simulated train speed between brackets.

Train Speed intervals [km/h]	Theoretical sleeper passing frequency range [Hz]	Experimental peak frequency [Hz]	Simulated peak frequency [Hz]
90-105	41.7 - 48.6	50	46 (100km/h)
105-115	48.6 - 53.2	56	-
115-125	53.2 - 57.9	59	55 (120km/h)
125-135	57.9 - 62.5	61.5	64.5 (140km/h)

TNO Internal 20/34

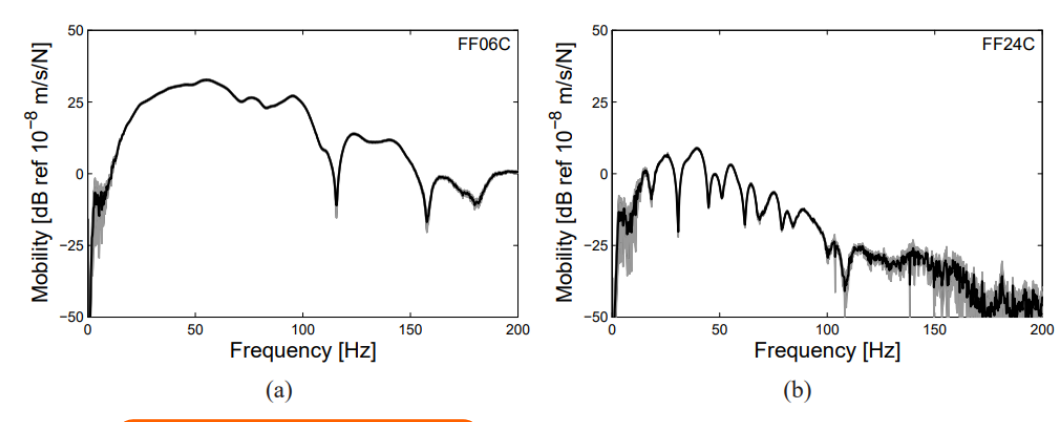


Figure 13: Average experimental transfer function (mobility line, black) and 95% credible interval (grey region) determined by 100 hammer tests at 6 and 24 meters from the tracks from [4].

#### 3.3 SLT

Figure 14 shows the median PSD obtained from the measurements (left y-axis) against the PSD force obtained from Ricardo (right y-axis) for the SLT train for different intervals of train speed (rows). Like for the VIRM train, no Ricardo simulation was available for the speed interval 105-115 km/h.

In the figure, the row of sensors closest to the source, at about 25 m distance, is used (MT30, MT31, MT32). If there is any correlation with the dynamic track loads it is most likely found in the sensors closest to the track. Figure 15 shows a comparison per sensor of the PSDs obtained per speed interval, while Figure 16 and Figure 17 provide a zoom on respectively the frequency content below 15 Hz and above 40Hz.

The considerations on the PSD spectra of the VIRM are also applicable to the induced vibration measured for passages of SLT train:

- In comparing the sensors amongst each other, the median PSD is in good agreement in some parts of the spectrum in up to 15 Hz and between 40-100Hz. Similarly, as for the VIRM, a different attenuation between 15-30Hz is observed which strengthens the hypothesis that is related to local conditions at the sensor or the tracks.
- For all sensors, a similar trend in amplitude and increase in frequency (shift to higher values with increasing train speed) is found. It is worth noting that the shape of the spectra between 15Hz and 40Hz shows a smaller dependency on the train speed.
- When the PSD of the dynamic load on the track resulting from the simulations (black line, right axis) is qualitatively compared with the output PSD, some similarities can be found in the relatively high-frequency range, but the peaks not always align. Different than the VIRM train type, multiple peaks are found in the frequency range above 40Hz.

TNO Internal 21/34

- As for the VIRM, a poor match is found between the PSD of the force and the PSD of the velocities for the remaining part of the spectra, especially where the largest frequency content of the measurement is found (8-15Hz). The experimental PSD shows in fact pronounced peaks which cannot be traced to peaks in the PSD of the force.

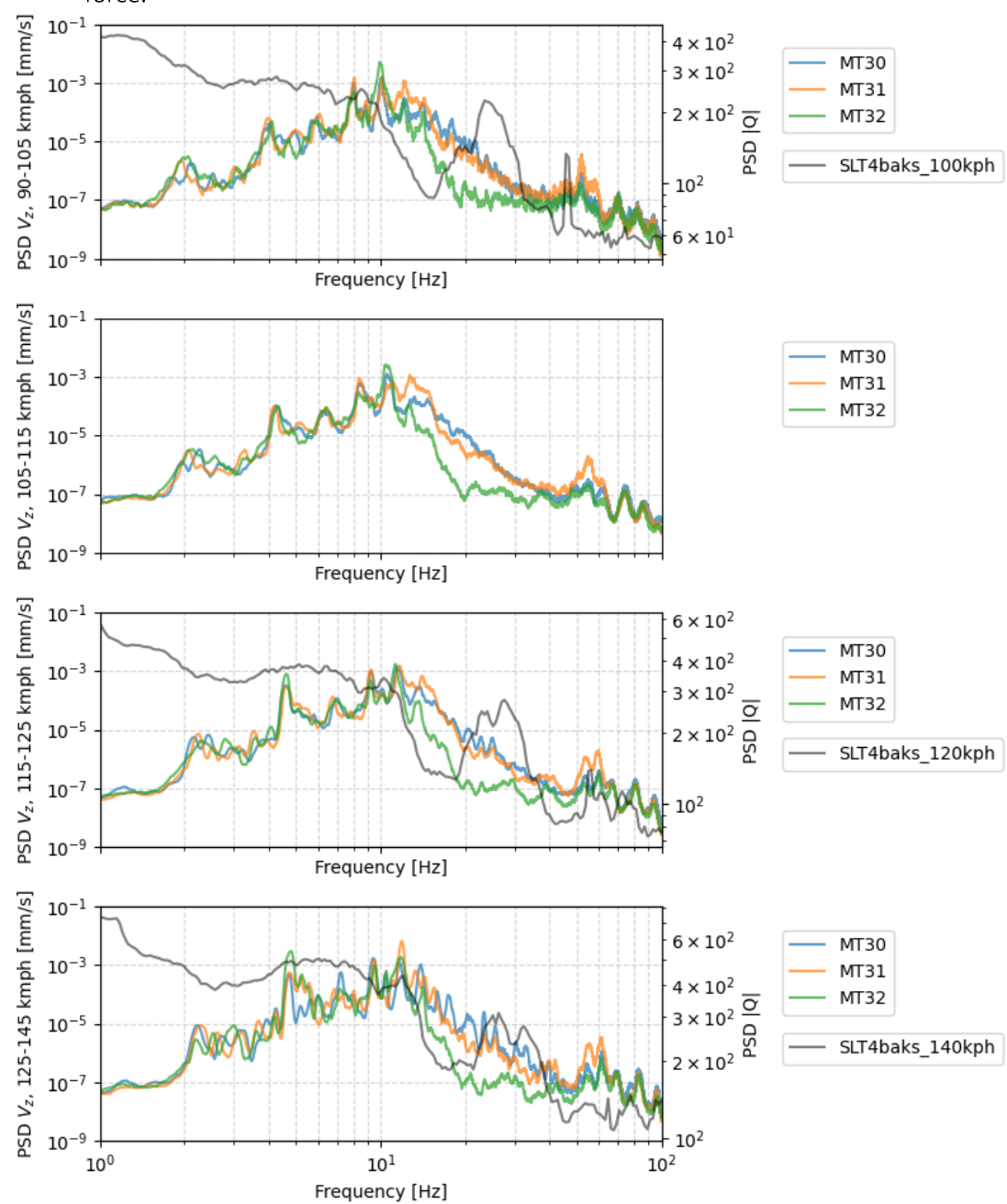


Figure 14: Median PSD of the vertical velocity obtained from the measurements (left y-axis) against the PSD force obtained from Ricardo (right y-axis, grey line) for the SLT train for different intervals of train speed (rows). Note that there was not a matching Ricardo simulation for the speed bracket 105-115 km/h.

TNO Internal 22/34

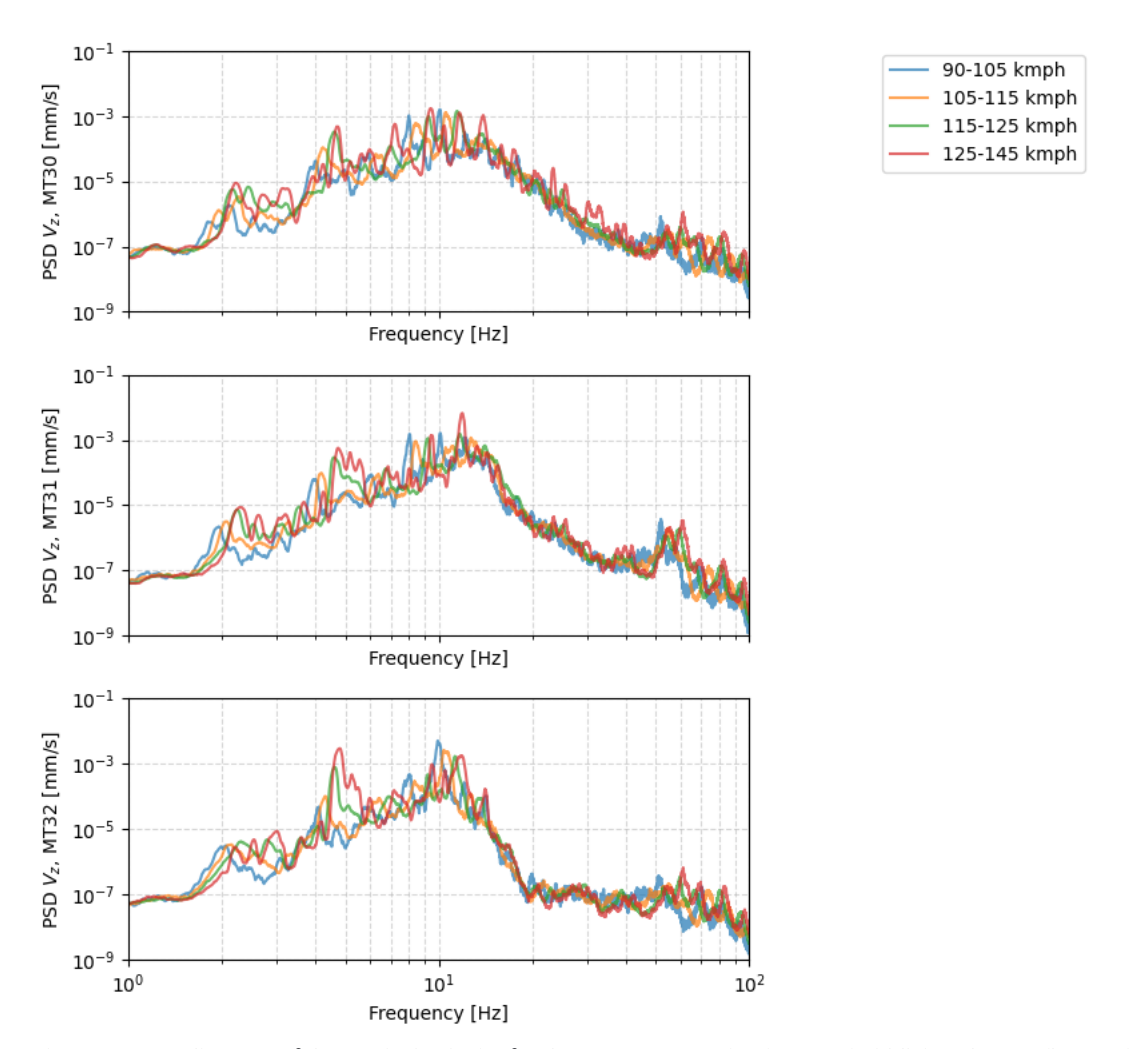


Figure 15: Median PSD of the vertical velocity for the sensors MT30 (top), MT31 (middle) and MT32 (bottom) for different SLT train speed intervals (colours).

) TNO Internal 23/34

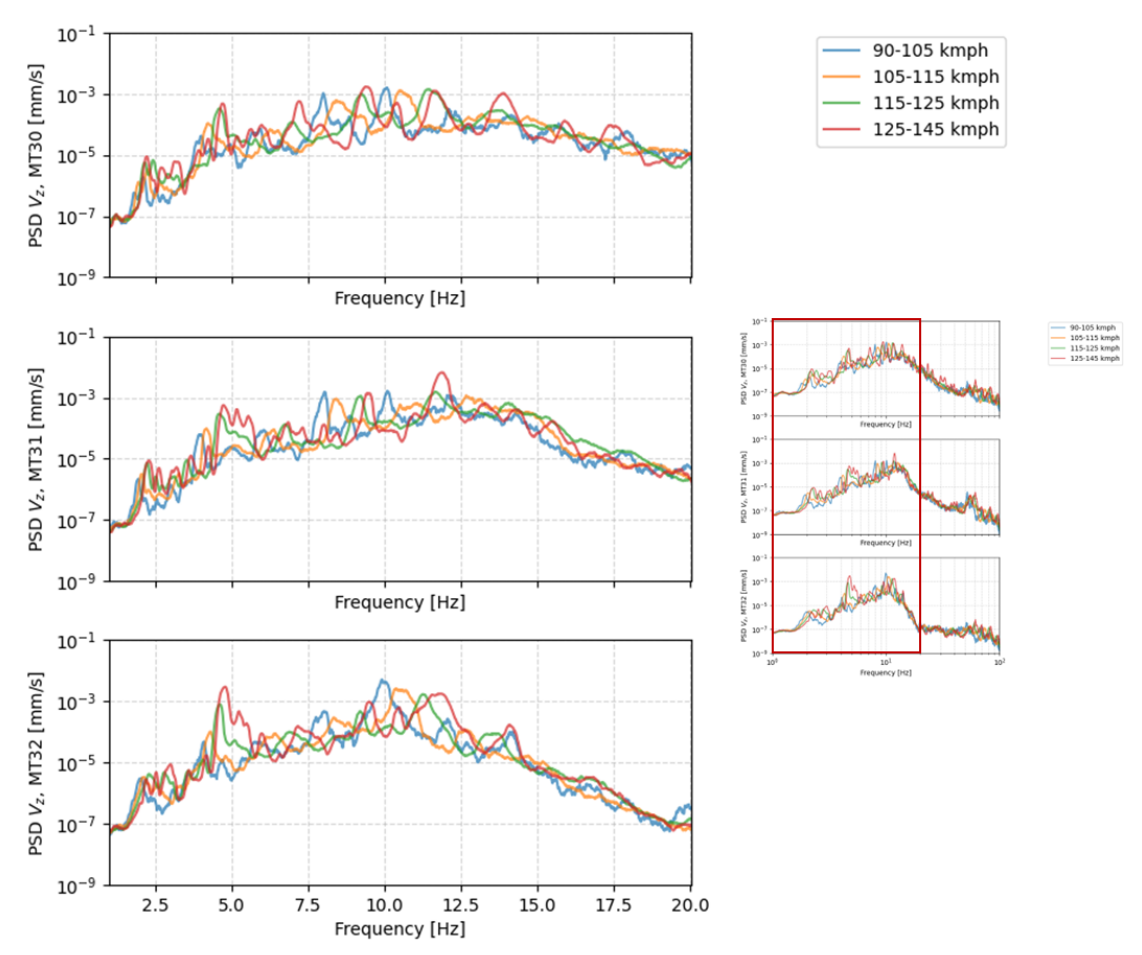


Figure 16: Median PSD of the vertical velocity for the sensors MT30 (top), MT31 (middle) and MT32 (bottom) for different SLT train speed intervals (colors) zoomed in the range 1-20 Hz (see thumbnail on the right).

) TNO Internal 24/34

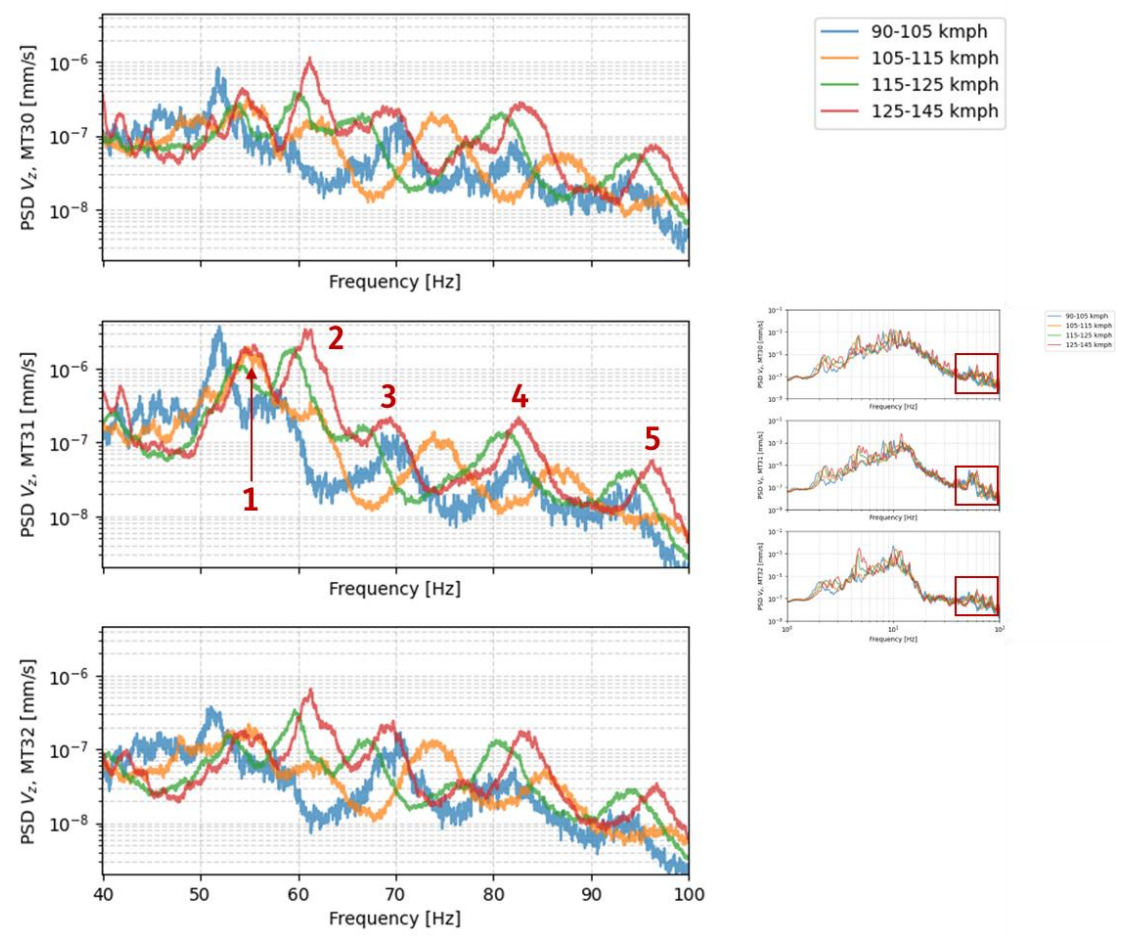


Figure 17: Median PSD of the vertical velocity for the sensors MT30 (top), MT31 (middle) and MT32 (bottom) for different SLT train speed intervals (colors) zoomed in the range 40-100 Hz (see thumbnail on the right). The peak number is indicated for the 125-135 km/h speed interval with red numbers.

When observing the high-frequency peaks in the median PSD of the individual sensors (Figure 17), each peak found for in a speed-interval can be related to corresponding peaks in the other train speed intervals, with a consistent increase in frequency. The estimated peak frequency for each speed interval and corresponding peak is presented in Table 5 while the peak id is presented in Figure 17 . In the table, the theoretical passing sleeper frequency is also indicated for the upper and lower bound of the speed interval.

Table 5: Theoretical vs Experimenta ak frequencies in the range of the sleeper passing frequency range obtained from the VIRM true per assuming 0.6m sleeper distance.

Train Speed intervals			Experimental frequency peaks [Hz]					
[km/h]	passing frequency [Hz]	1	2	3	4	5		
90-105	41.7 - 48.6	43-47	52	57.3	70.5	82.5		
105-115	48.6 - 53.2	50	55	61.7	74.4	87		
115-125	53.2 - 57.9	54	59.7	67	81	94		
125-135	57.9 - 62.5	55.4	61	69	82	96		

TNO Internal 25/34

#### 3.4 All train types

To investigate the effect of local soil and tracks effects on the measured velocity PSD, the PSD obtained using a) different train speeds and b) different train types are plotted separately per sensor in Figure 19. The individual lines can be found in Appendix A.

The figure shows that, as discussed already for the VIRM and SLT train types, there is a part of the output spectra (10-30 Hz) which shows a negligible influence on the train speed and is relatively insensitive to the train type.

In the relatively low-frequency range and high frequency range, a clear difference is found per train type:

- The VIRM train shows a contribution between 1 and 2 Hz in the form of a local peak that the other trains don't have.
- The freight train has a remarked contribution in the range 3-6Hz compared to the passenger trains.
- In the relatively high-frequency range, a difference is observed between freight, passenger trains and locomotive. A peak around 41 Hz is found for the freight-trains which is close to the theoretical sleeper passing frequency for 80 km/h speed, the most frequently found speed during the measurement campaign for freight trains (although for only 60 passages).
- Peaks in the VIRM and SLT are also found close to the theoretical sleeper passing frequency, although their frequency tends to be higher when compared to the theoretical sleeper passing frequency as well as the peak frequency in simulations.

) TNO Internal 26/34

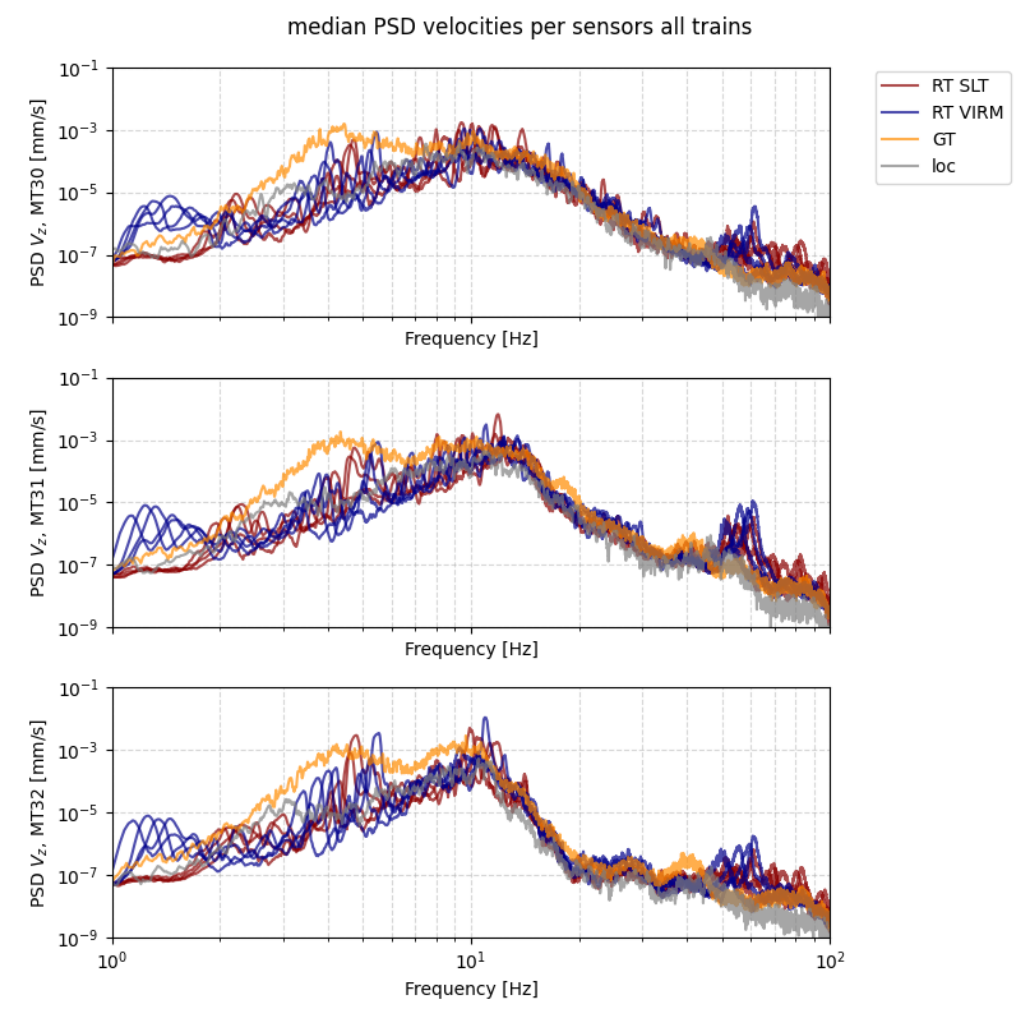


Figure 18: Median PSD of the vertical velocity for the sensors MT30 (top), MT31 (middle) and MT32 (bottom) for SLT (red), VIRM (blue), locomotive (grey) and freight train (orange). For the SLT and VIRM, multiple lines of the same color indicate different train speeds.

TNO Internal 27/34

## 4 Conclusions & Recommendations

In 2018, a measurement campaign at the Schalkwijk location has been performed in which velocity has been recorded at 3 distances (25, 49 and 72 meters approximately), in 3 sensors per distance spaced 25 meters apart.. Later, Ricardo [1] performed numerical simulations of a detailed train model passing on a track which is modelled after the same track of the Schalkwijk measurement campaign. These simulations were performed for different types of passenger trains, freight trains and locomotives and at different train speeds.

This report addressed the question whether the dynamic axle loads on the rail have a direct correspondence with measurements in the field at some distance from the track in terms of frequency content. To this end, the measurement data recorded in field sensors in Schalkwijk has been compared the numerical simulations performed by Ricardo in the frequency domain (PSD).

The main conclusions can be summarized as:

- In the low frequency range (<5 Hz) there is no resemblance in the spectral shape between field recordings and track loads. This can be explained by the fact that low frequencies are strongly attenuated from track to the soil as evidenced by transfer functions from literature.
- In the low frequency range (<12 Hz) the field measurements show local peaks of low amplitude in the spectrum that depend on train speed. Such peaks are not found in the dynamic track loads from the simulations.
- In the mid-frequency range (12-35 Hz) the field measurement spectra show little variation with train type and train speed. Also, the dip in the spectrum of numerically computed track loads is not visible in the field recordings and the spectral slope does not match well either. Difference in recordings at the same track distance shows some variation in the spectrum, suggesting the spectral shape may be largely determined by specific track and soil conditions.
- In the relatively high frequency range (>35 Hz) peaks are observed in the field measurements that depend on train speed. Such peaks are also found in the simulated dynamic loads. However, the frequency of the measured peaks tends to be higher than the simulations peaks with the exception of train velocity 120 km/h. The simulated peaks seem to be related to the sleeper distance, but the measured peaks tend be at higher frequencies than the sleeper distance. It is unclear what is the cause of this. Also, the simulated peaks decrease in amplitude with train speed, and go from narrow to wider, while the peaks in the measurements are relatively constant in amplitude and have similar width.

The conclusions show that dynamic axle load frequency spectra are not directly relatable to vibrations at (25m) distance from the track. This makes it difficult to assess the effect of mitigations at the axle-track level on vibrations at some distance from the track.

TNO Internal 28/34

This finding is likely due to the fact that, in a real train, dynamic loads are generated at multiple axles simultaneously as they move along the track. These loads create waves in the soil at various points along the track, which eventually converge at a given location in the field. Additionally, in Ricardo's simulations, only individual cars or locomotives are modeled, rather than entire trains. Also, in the simulations of Ricardo, individual cars or locomotives are modelled, but not the full vehicles.

To better understand the relation between dynamic axle forces and field vibrations, it is recommended to use the STEM tool to model the Schalkwijk situation. The detailed simulations in [1] can be used to calibrate the train model and dynamic axle loads. The output of the STEM tool can be compared with the field measurements in Schalkwijk to determine if similar conclusions are arrived at. The complex system can then be simplified to understand different effects (such as the contribution of the effect of moving load without rail irregularities and sleepers, the effect of sleepers, the effect of rail irregularity, etc.).

TNO Internal 29/34

#### **5** References

- [1] Ricardo, "Simulaties van trillingsbelasting op het spoor," 2023.
- [2] W. P., The use of the fast Fourier transform for the estimation of power spectra: A method based on time averaging over short, modified periodograms, vol. 15, IEEE Trans. Audio Electroacoust, 1967, pp. 70-73.
- [3] R. Blackman and J. Tukey, The measurement of power spectra, New York: Dover Publications, 1958.
- [4] H. Verbraken, G. Lombaert and G. Degrande, "Experimental and numerical determination of transfer functions along railway tracks," in *Proceedings of the 9th National Congress on Theoretical and Applied Mechanics*, Brussels, 2012.

) TNO Internal 30/34

### **6** Signature

Delft, May 2025

Ir. D. Moretti Author

N. Gireesh Project Leader

Ir. M. van Roermund Research Manager Reliable Structures

) TNO Internal 31/34

#### Appendix A

In this appendix, the figures of all power spectral densities of the measured velocities for different train passages are reported for:

- RT VIRM (RT=reizingerstrain, i.e. passenger train), Figure 19.
- RT SLT, Figure 20.
- GT (Goederentrain, i.e. freight train), multiple types, Figure 21.
- Loc (Locomotive), unknown configuration, Figure 22.

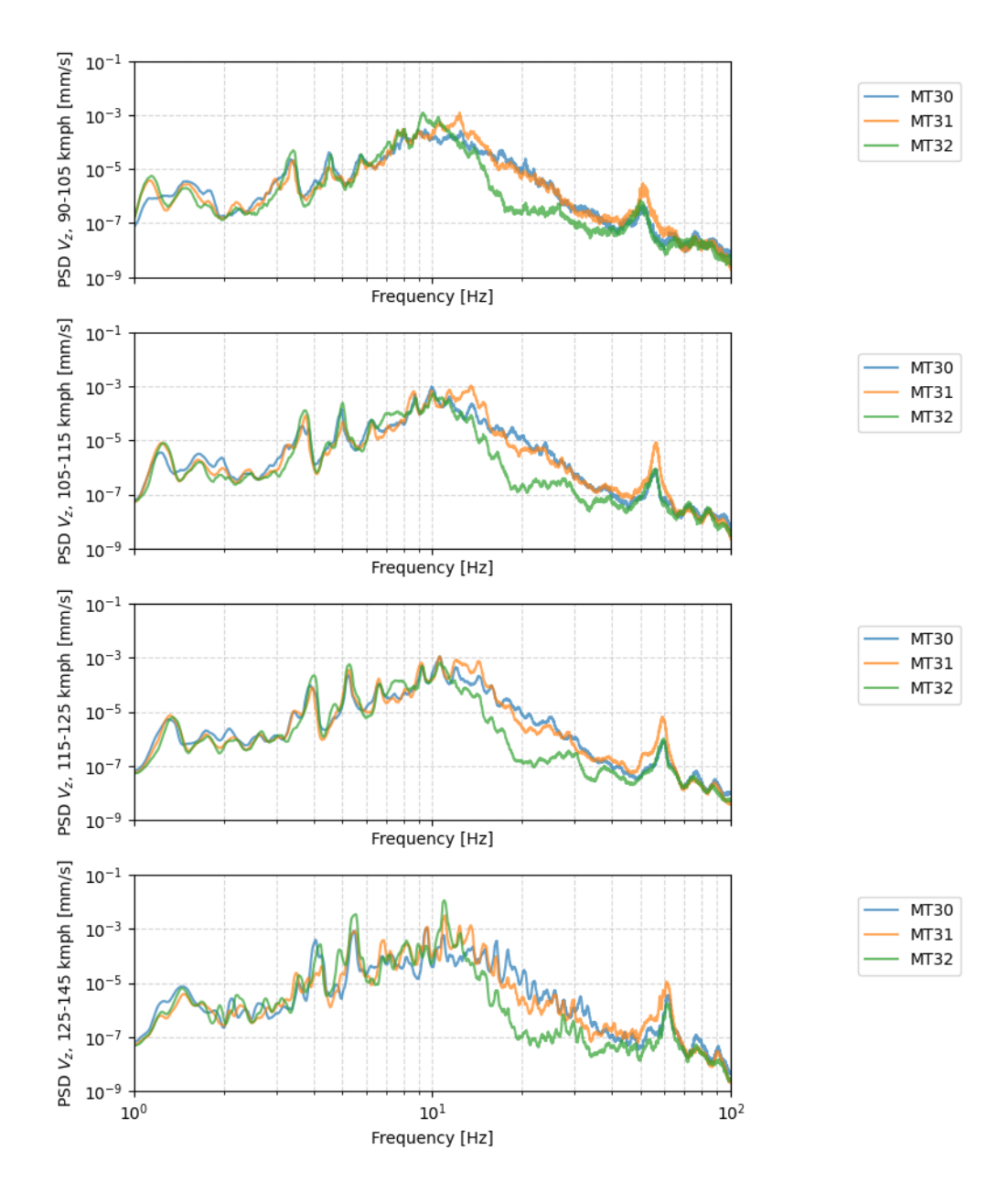


Figure 19: Median PSD of the vertical velocity obtained from the measurements for the VIRM train for different intervals of train speed (rows). Each row provides multiple sensors located at the 25m distance from the track (MT30, MT31, MT32).

) TNO Internal 32/34

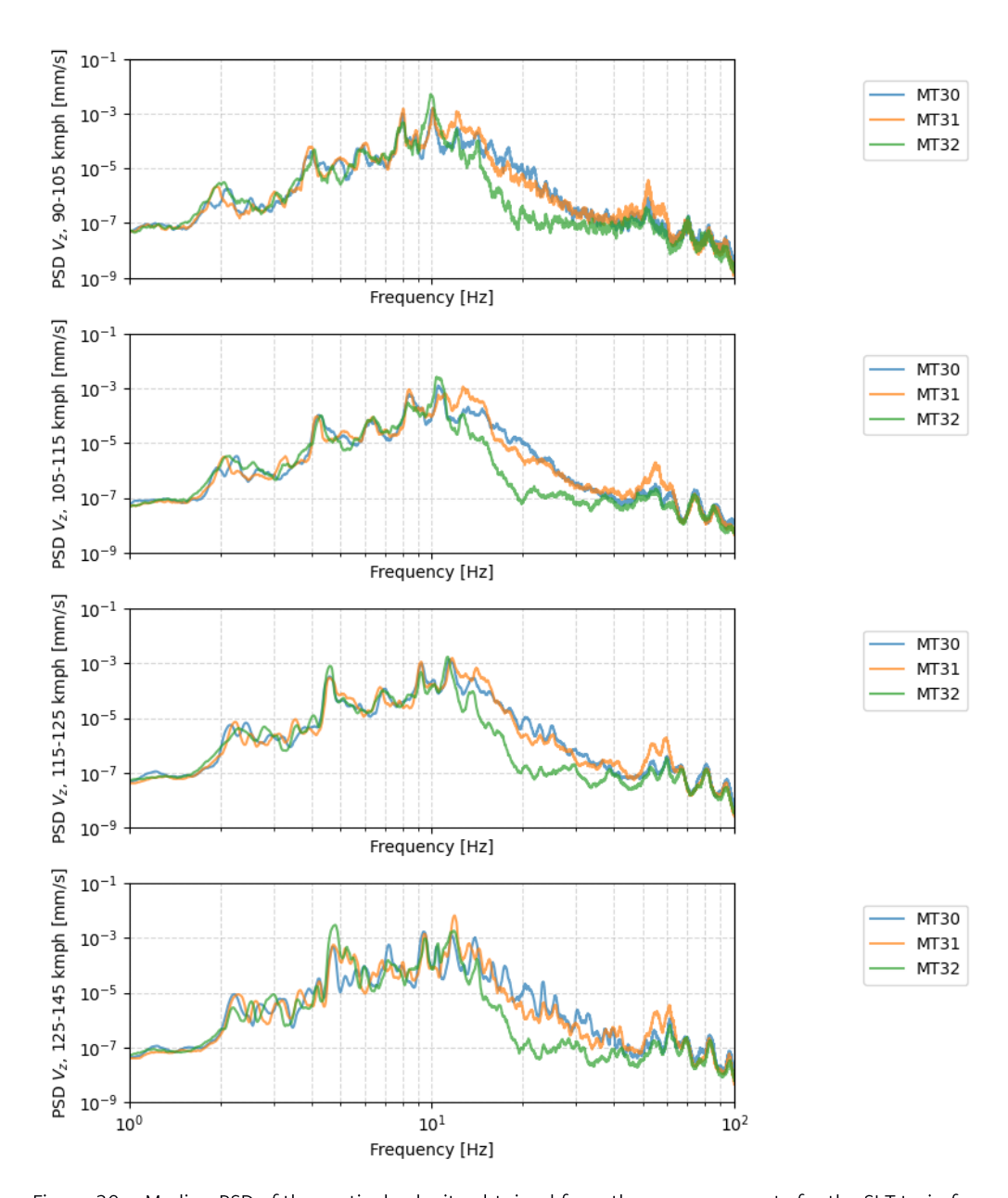


Figure 20: Median PSD of the vertical velocity obtained from the measurements for the SLT train for different intervals of train speed (rows). Each row provides multiple sensors located at the 25m distance from the track (MT30, MT31, MT32).

) TNO Internal 33/34

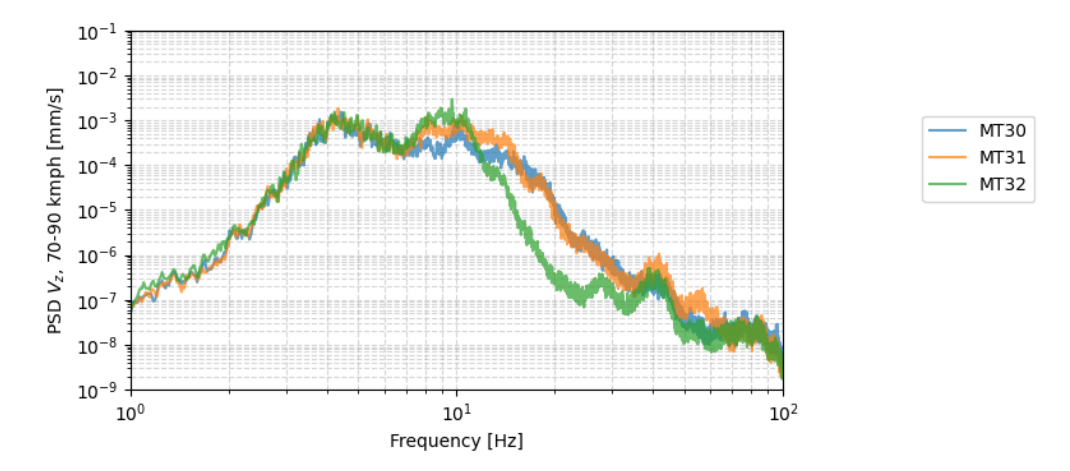


Figure 21: Median PSD of the vertical velocity obtained from the measurements for the GT train for multiple sensors located at the 25m distance from the track (MT30, MT31, MT32) for train speeds between 70 to 130 km/h.

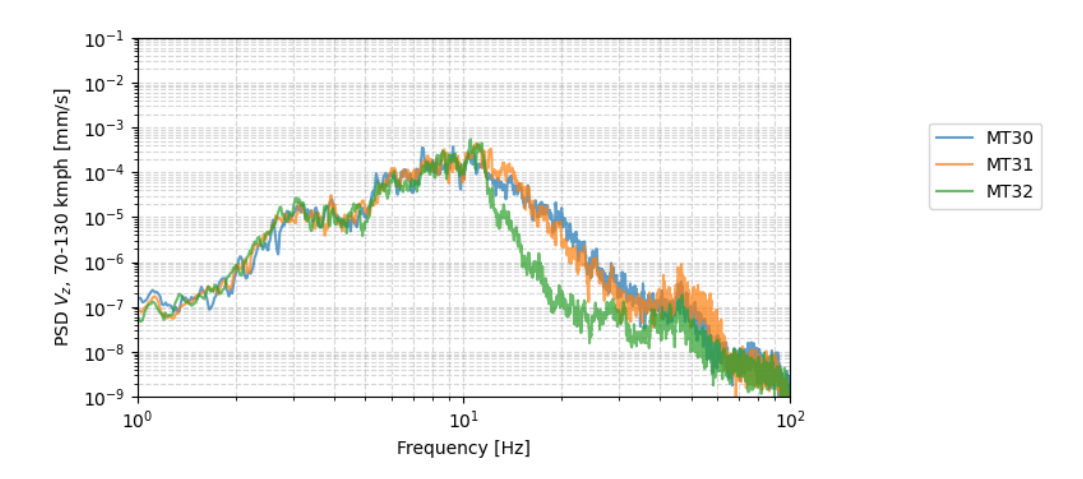


Figure 22: Median PSD of the vertical velocity obtained from the measurements for the Loc train for multiple sensors located at the 25m distance from the track (MT30, MT31, MT32) for train speeds between 70 to 130 km/h.

) TNO Internal 34/34

Mobility & Built EnvironmentMobility & Built EnvironmentMobility & Built Environment

Molengraaffsingel 8 2629 JD Delft www.tno.nl

